Effect of Accelerated Aging on Microstructure and Initiation of Vapor-Deposited PETN Films

Robert Knepper, Will Bassett, Christina Crawford, David E. Kittell, Michael P. Marquez, Jennifer Quinn, Alexander S. Tappan, and David L. Damm

Explosives Technology Group
Sandia National Laboratories
Albuquerque, NM 87185

Abstract. Vapor-deposited PETN films undergo significant microstructure evolution when exposed to elevated temperatures, even for short periods of time. This accelerated aging impacts initiation behavior and can lead to chemical changes as well. In this study, as-deposited and aged PETN films are characterized using scanning electron microscopy and ultra-high performance liquid chromatography and compared with changes in initiation behavior measured via a high-throughput experimental platform that uses laser-driven flyers to sequentially impact an array of small explosive samples. Accelerated aging leads to rapid coarsening of the grain structure. At longer times, little additional coarsening is evident, but the distribution of porosity continues to evolve. These changes in microstructure correspond to shifts in the initiation threshold and onset of reactions to higher flyer impact velocities.

Introduction

Shock sensitivity in high explosive materials is often highly dependent on microstructure. While parameters like bulk density have been studied extensively, distributions of grain sizes or porosity can also have a significant impact on initiation threshold, critical diameter, corner-turning ability, and other behaviors.[1-3] As an explosive material ages, diffusional and chemical processes can lead to changes in the microstructure, which can in turn impact their performance. Pentaerythritol tetranitrate (PETN), despite being widely used in both mining and military applications, is known to be susceptible to changes in both microstructure and performance due to aging.[4-10]

Vapor-deposited films provide a useful model system to study the effects of aging on microstructure and performance in explosives. Physical vapor deposition provides precise control over sample geometry and consistency in initial microstructure and morphology. Vapor-deposited films also allow for detailed studies of initiation behavior using the High-Throughput Initiation (HTI) experiment developed at Sandia National Laboratories.[11] The HTI experiment has generated a wealth of thin pulse, sub-millimeter shock initiation data for a variety of vapor-deposited explosive films and can track the growth of chemical reactions leading to detonation on temporal and spatial scales that were not previously attainable. These data have shown that reactions in PETN films can grow to detonation at sub-100 μm

thicknesses following impact by 25 μm thick Parylene-C flyers at sufficient velocities. Using vapor-deposited films at these length scales also allows for collection of high-resolution scanning electron microscopy (SEM) images that can capture details of the microstructure over the full thickness of the film.[12-14] This provides a reasonable length scale for importing microstructure data to shock physics hydrocodes, like CTH, to enable direct comparison of experiments with mesoscale simulations.[15-17]

In this paper, we use vapor-deposited PETN as a model system to examine the effect of accelerated aging at various time-temperature conditions on the evolution of microstructure, chemistry, and initiation behavior. Vapor-deposited films are exposed to elevated temperatures for time periods ranging from a few hours to a month. Both top surface and cross-section microstructures are characterized using SEM to observe how they evolve with time at elevated temperatures, and changes in chemistry are characterized using ultra-high performance liquid chromatography (UPLC). Growth to detonation under shock impact of both as-deposited and aged samples are characterized using the HTI experiment, and relationships between the evolution of microstructure or chemistry and the changes in performance are evaluated. This combination of material and performance characterization improves our understanding of the mechanisms that control shifts in performance with aging in PETN.

Experimental Methods

PETN films were deposited in a custom-designed high-vacuum chamber operating at a base pressure of approximately 10^{-6} Torr. PETN powder was loaded into an effusion cell deposition source, heated under vacuum, and deposited *via* thermal evaporation. Shadow masks defined the geometry of the deposited films. Samples for microstructure characterization were deposited in a 7 mm square geometry onto 10 mm × 10 mm (100) silicon substrates (American Precision Dicing, San Jose, CA). Samples for HTI experiments were deposited on a 2 mm diameter spot on 6.35 mm diameter, 3.18 mm thick poly(methyl methacrylate) substrates (Spartech Polycast, Poly II MIL-P-5425). Prior to PETN deposition, a 2 μm aluminum layer was deposited using an electron beam deposition source in the same vacuum chamber. Additional details of the deposition process are described elsewhere.[18] To reach the desired film thickness, multiple deposition runs were sometimes required. Some samples were thermally treated by placing inside of a sealed aluminum sieve pan, which was placed in an oven (Thermotron, Holland, MI) for times ranging from 4 hours to 33 days and temperatures ranging from 50° – 70°C. Details of the specific accelerated aging conditions tested can be found in the Results section.

Microstructure characterization was performed using scanning electron microscopy with a Zeiss GeminiSEM 300. All images were collected with an accelerating voltage of approximately 1 kV, and PETN surfaces were coated with a thin layer of iridium prior to imaging to mitigate surface charge build up. Top surface images were collected at a variety of fields of view and a 2048 x 1536 image resolution. Cross section samples were prepared by scoring and fracturing the silicon substrate. Images of the fracture cross section were taken at the same image resolution as the top surface images with fields of view of ~100 – 150 μm. Some cross sectioned samples were ion polished using a Hitachi IM 4000 Plus argon ion milling system to enable characterization of the distribution of porosity. Since PETN could be damaged by excessive ion bombardment, samples were held in a cryogenic stage at -60°C while milling to minimize beam damage. Films were typically milled with an accelerating voltage of 4 kV, a beam current of approximately 25 – 30 μA, and using a ± 30° stage swing. High-resolution images of the ion-polished cross sections were obtained using a 10 nm pixel size.

In addition to SEM characterization, stylus profilometry (Bruker Dektak XT) was used to measure film thicknesses and quantify surface roughness. Film thicknesses were measured using single line scans that included parts of the substrate to use as a reference. For roughness measurements, a series of scans with 1 μm spacing between scan lines was performed over an approximately 1 mm^2 area near the center of the film. These data were analyzed using the Vision 64 software package to determine average roughness values.

The HTI experiment was used to study shock initiation behavior in the PETN films. This system utilizes laser-driven 25 µm thick Parylene-C flyers to sequentially shock an array of samples while using photonic Doppler velocimetry (PDV) diagnostics to monitor sample response at the film-substrate interface, as shown in Fig. 1. The laser-driven flyer was based on a similar system developed in the Dlott laboratory at the University of Illinois, Urbana-Champaign,[19,20] with some modifications; see Knepper *et al*[11] for details of the experiment setup and analysis of the PDV data.

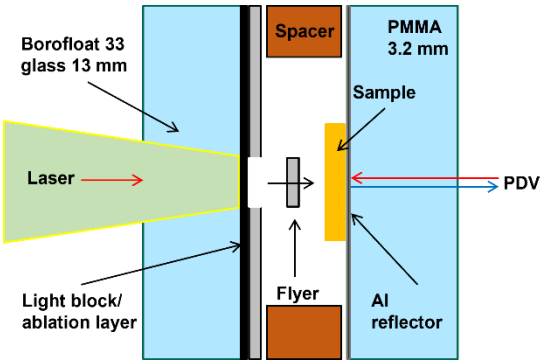

Fig. 1. Cross-sectional diagram of the laser-driven flyer and sample setup in the high-throughput initiation experiment.[11]

Ultra-high performance liquid chromatography electrospray ionization quadrupole time-of-flight mass spectrometry (UPLC-ESI-QTOF-MS, Waters XEVO G2-XS) was performed on PETN films as-deposited, aged for 1 day at 60°C, and aged for 2 weeks at 60°C to identify impurities or decomposition products present and their relative quantities. A gradient UPLC elution method was used according to Table 1.

The LC run time was thirteen minutes, with the MS data collection ending after five minutes from the start of the 2 µL sample injection. Since PETN was the primary species in these samples, a solvent delay was added during each run so that when PETN eluted, that peak's material was shunted to waste and the MS detector turned off. This technique allows for better detection of the minor homologs and potentially degraded species in the samples, as electrospray ionization is a competitive, concentration-dependent ion formation process.

Table 1. Gradient UPLC elution method. Solvent A: 18 MΩ cm deionized water with 10 mM ammonium acetate. Solvent B: LC-MS grade acetonitrile (Fisher Optima).

Run Time (min.)	Solvent A (%)	Solvent B (%)
0.3	40	60
5.0	10	90
10.0	10	90
10.1	40	60
20	40	60

The QTOF-MS system was calibrated from 50-1000 Da using a sodium formate calibration solution. The calibration passed with a 0.3 ppm (0.1 mDa) mass accuracy in the negative ionization, sensitivity mode. A lock mass compound (leucine enkephalin (LeuEnk) at 554.2615 Da) was also used during each sample collection period to maintain mass accuracy during the sample period. Measured mass resolution of 30,000 was recorded for LeuEnk at 554.2615.

External calibration was performed using a TriPEON sample with an assumed purity of nearly 100% and a DiPEHN sample with an assumed purity of 90%, both based on chromatographic purity. A PETriN calibration sample was approximately 50% pure. Stock standards of each material were created at 25, 50, and 100 ppm, and three-point calibration curves were constructed using these samples for each of the three homolog materials and for PETN. The sample run was constructed by bracketing the calibration samples and the accelerated aged samples using a wash sample (LC-MS grade acetonitrile), a PETN check standard (for quality control), and a procedural blank (to detect any matrix effects).

UPLC-MS data were analyzed, and plots were generated using Waters MassLynx 4.2 software. For each homolog of interest, extracted ion chromatograms (XIC) at an analyte-specific adduct mass were used to find the integrated area under that peak for quantitation. Table 2 provides the relevant details.

Table 2. Retention times, XIC mass used for quantitation, and the adduct of that species.

Compound	Elution Time (min)	XIC mass	Adduct (nominal mass)
PETriN	1.2	330.18	$[M+CH_3COO]^-$
DiPEHN	2.85	583.06	$[M+CH_3COO]^-$
TriPEON	3.67	791.09	$[M+CH_3COO]^-$

Results

Representative SEM images of the top surfaces of as-deposited and aged films are shown in Fig 2. The different aging time and temperature values represent all of the conditions investigated in this study. Multiple images were collected at several different fields of view (100, 250, and 500 µm, only 100 µm images are shown here) to qualitatively assess the evolution of microstructure with aging. Figure insets display fracture cross sections at each condition. Scale bars shown in the lower right image are representative of the entire array of images. As-deposited PETN films had a lateral grain size on the order of 1 µm; the fracture cross section shows a columnar structure in which the grains are extended to a few tens of microns in the direction of growth. Significant grain growth occurred following even short amounts of time at elevated temperatures. As samples were aged for longer periods of time, there did not appear to be much continued grain growth. Instead, the sharp edges of grains started to dull, and the columnar structure became less distinct. Following one month at 70°C, individual grains were difficult to identify, and all evidence of a columnar structure had disappeared.

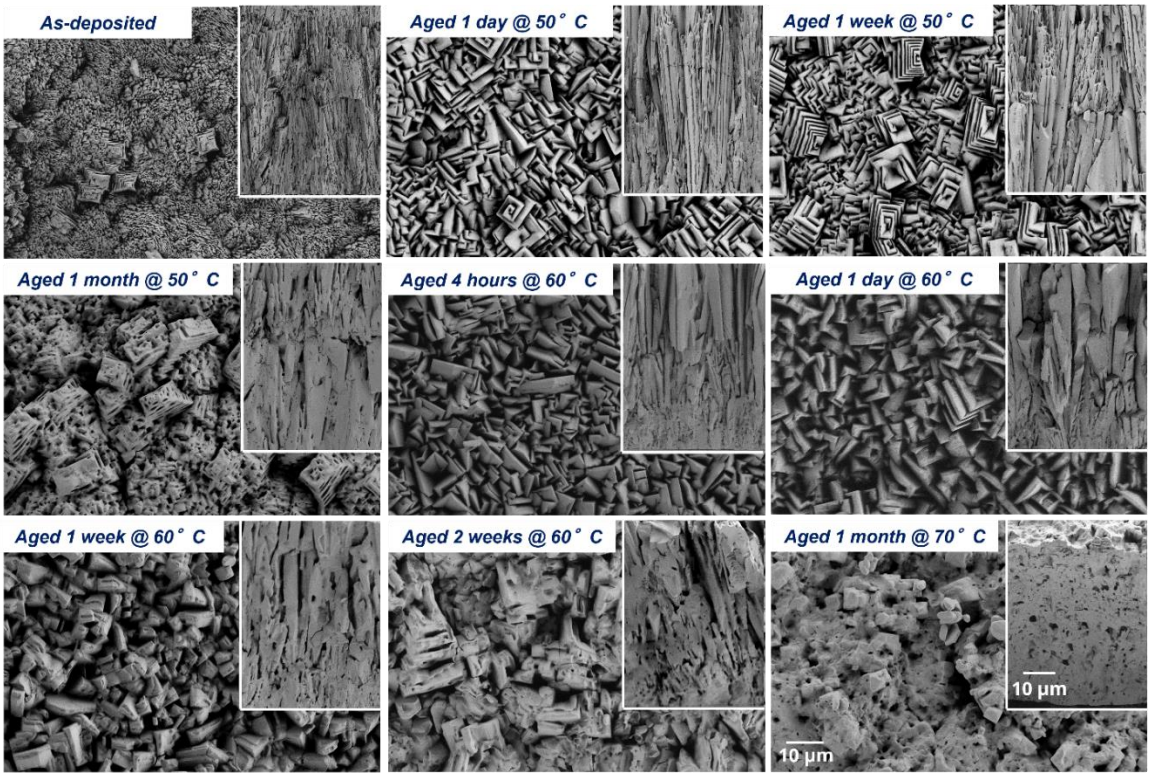

Fig. 2. SEM images of the top surfaces and fracture cross-sections (inset) of as-deposited and aged PETN films. The field of view of each top-surface image is 100 µm. Scale bars in the bottom right are representative of all images.

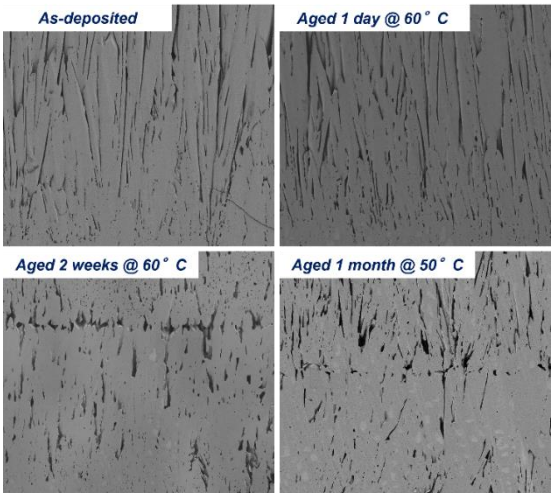

Fig. 3. SEM images of ion-polished cross sections of PETN films (a) as-deposited, (b) aged 1 day at 60°C, (c) aged 2 weeks at 60°C, and (d) aged 1 month at 50°C. All images display a 90 µm field of view.

Ion-polished cross-sections were collected for as-deposited films, along with those aged for 1 day at 60°C, 2 weeks at 60°C, and 1 month at 50°C; representative images are shown in Fig. 3. The field of view for all images shown is 90 µm, and several images were collected at each aging condition. These images provide a clear view of the distribution of porosity in the films. The as-deposited and aged 1 day at 60°C cross sections look similar, with smaller pores near the substrate interface (bottom) and long, narrow pores extending in the direction of film growth. Following aging for 2 weeks at 60°C or 1 month at 50°C, some smaller pores near the substrate interface remain, but the longer pores do not extend as far in the direction of growth, creating a somewhat less anisotropic distribution of porosity. In addition, breaks between deposition runs can be seen clearly in these films as a roughly horizontal region with increased porosity.

Average surface roughness was also measured for samples at each condition using stylus profilometry. Surface roughness did not appear to change significantly with aging, generally spanning the range observed for different as-deposited samples (about 1.4 – 2.2 µm) with no clear trends with either aging time or temperature.

The UPLC data were analyzed and categorized according to each of the three time-temperature conditions studied: as-deposited (i.e., the control samples for the accelerated aging experiment), the 1 day/60°C, and the 2 weeks/60°C (i.e., 14 days). Each of the samples in these categories was then analyzed for homolog content and concentration across both the retention time and homolog mass range. Fig. 4 displays overlaid traces for representative samples from each aging condition centered on peaks corresponding to PETriN (Fig. 3a) and TriPEON (Fig. 3b). In each case, the data show a monotonic decrease in peak height and area with increasing aging time.

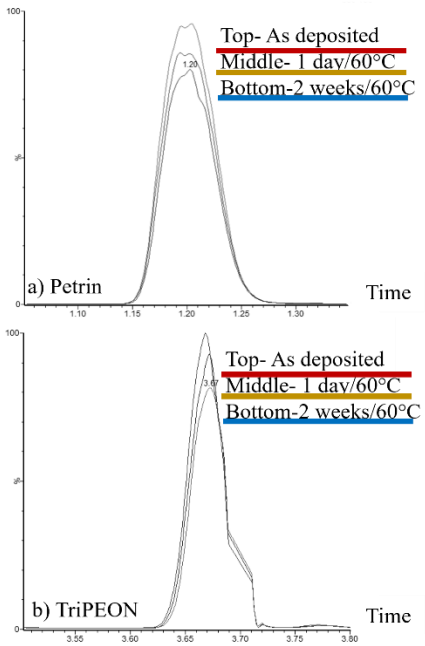

Fig. 4. XICs of a) PETriN (1.2 min.; 330.18 Da) and b) TriPEON (3.67 min.; 791.09 Da) from representative samples in each category: As deposited/control (underlined in red, top trace); 1 day/60°C (underlined in gold, middle trace); and 2 weeks/60°C (underlined in blue, bottom trace).

Fig. 5 shows similar data to that of Fig. 4 but with the DiPEHN homolog of PETN. Fig. 5a shows the overlaid traces of three representative samples from each of the three categories, but now, Fig. 5b shows a boxplot of the DiPEHN concentrations measured across all samples from each category. While the variance of the 1 day/60°C samples

(shown in gold) is leading to higher spread and overlapping confidence intervals with the 14-day samples, there is enough distinction between the as-deposited/control samples and the aged samples to see a statistically significant reduction in the DiPEHN concentration (at α=0.05) as a function of time and temperature. Levene's test[21] was used to check for homogeneity of variance across samples. The test verified the assumption that the sample variances were equal.

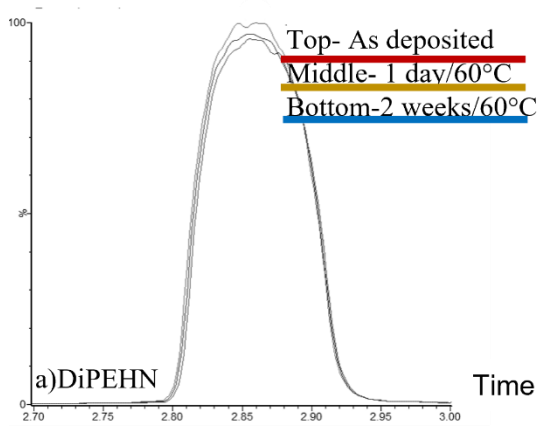

Fig. 5. a) XICs of DiPEHN (2.87 min.; 583.06 Da) from representative samples in each category: As-deposited/control (underlined in red, top trace); 1 day/60°C (underlined in gold, middle trace); and 2 weeks/60°C (underlined in blue, bottom trace), and b) a box plot showing the sample concentrations for all the samples across each category (n=8, 5, and 6, respectively).

As discussed in Knepper *et al*,[11] given the large number of PDV datasets generated from high-throughput testing, it is easier to compare trends in the data by focusing on a single metric rather than the details of each trace. As such, in Fig. 6, we plot the peak particle velocity following flyer impact as a function of impact velocity. Fig. 6 shows data from 100 µm thick PETN films, with separate plots for samples aged at 50°C and 60° or 70°C. The simulated inert response shown in each figure was generated using 1D simulations in the shock hydrocode CTH, as described in detail elsewhere.[11]

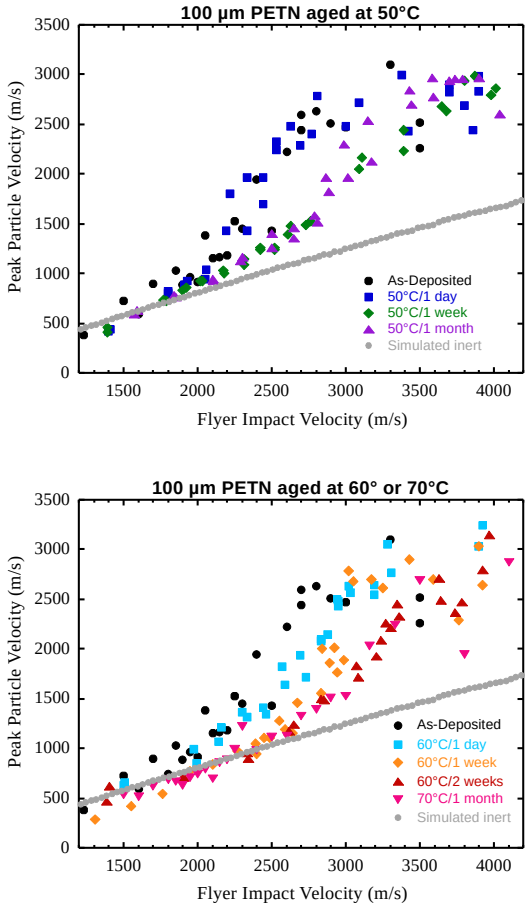

Fig. 6. HTI results on 100 µm PETN films (a) aged at 50°C and (b) aged at 60° or 70°C.

For the films aged at 50°C, the data from samples aged for 1 day appeared similar to that of the as-deposited films, initially following the predicted inert response before deviating at flyer impact velocities above 2200 m/s and leveling off around 2800 m/s. Data from films aged for 1 week

and 1 month likewise appear similar to each other. The data for these samples display a shift in where deviation from the inert simulations occurs, with the experimental data remaining just above the simulated inert line until flyer impact velocities above ~2800 m/s. While there was considerable scatter in these data at higher impact velocities, the data appeared to level off above ~3400 m/s.

For films aged at 60°C, a small but noticeable change in performance was observed for samples aged for only 1 day, with a clear shift in where the data level off compared to as-deposited samples but little change in the first deviation from the predicted inert response. Larger shifts were observed following 1 week and 2 week aging times. Interestingly, the data from films aged for 1 month at 70°C data were indistinguishable from the 60°C/2 week aging condition.

Discussion

Significant changes in microstructure occur in PETN films following even short amounts of time at elevated temperature. Early in the aging process, grain coarsening appears to be the main mechanism driving changes in microstructure. Following longer times at elevated temperature, little additional grain growth is observed, and continued evolution of the microstructure appears to be occurring through changes in the porosity.

A trend in the UPLC data emerged, as shown in Figs 4 and 5, of decreasing homolog content as a function of aging time at temperature. The three homologs examined across the PETN homolog mass range: the lower molecular weight homolog PETriN ($C_5H_9N_3O_{10}$ at M=271.03Da with an $[M+CH_3COO]^-$ adduct at 330.04), middle-range molecular weight DiPEHN ($C_{10}H_{16}N_6O_{19}$ at M=524.05 Da with an $[M+CH_3COO]^-$ adduct at 583.06), and the higher molecular weight TriPEON ($C_{15}H_{24}N_8O_{26}$ at M=732.08 Da with an $[M+CH_3COO]^-$ adduct at 791.09), all showed decreasing peak areas with accelerated aging time/temperature. This trend may be due to mass loss; the effect is seen as a peak area decease, which correlates to a decrease in the measured concentration for that homolog. A brief survey of several samples in each category did not indicate any new species were increasing in peak area (i.e., "growing in"). If this was the case, it may indicate conversion to lower mass species due to degradation. Gaseous species may also be produced if the material can partially sublime at these aging conditions, but this phenomenon would not be apparent in the LC-MS analysis.

Data from HTI experiments can generally be interpreted as follows. At low impact velocities, reactions typically do not occur fast enough to contribute significantly to the pressure at the shock front; as such, measured peak particle velocities generally agree with the predicted inert response. As impact velocity increases, chemical reactions start to occur fast enough to impart significant extra energy on the timescale of the shock – here, experimental peak particle velocities begin to deviate from the predicted inert response, allowing us to identify the onset of reaction. Particle velocity typically increases rapidly with increasing impact velocity in this regime, as chemical reactions build more quickly and contribute more energy to the shock front. At some point, particle velocity stops increasing with additional increases in flyer impact velocity; we interpret this as the transition to a full detonation. Note that the duration of a supported shock in PETN with a 25 µm Parylene-C flyer (roughly 12 ns) is such that the inert simulations predict a rarefaction will catch up with the shock front at a distance of approximately 80 µm into the PETN film. This means that the shock is supported through most of the thickness of these 100 µm samples, but the pressure at the shock front will start to decay near the film-substrate interface if reactions do not occur fast enough in the PETN film to contribute energy to the shock.

The data in Fig. 6 show that PETN films generally become less sensitive with aging. At shorter aging times, films aged at 50°C show minimal changes from the baseline data, while those aged at 60°C had a more significant shift in initiation threshold. Little change was seen in the onset of reactions in either case. Larger shifts in performance were observed for films aged for longer times. In these samples, both the onset of reaction and initiation threshold shift to higher flyer impact velocities.

Ion-polished cross-section images can be thresholded and binarized to segment solid regions from pores, which allows for quantification of various microstructure metrics. Threshold values

for segmentation were determined using the Kittler-Illingworth "Minimum Error" method.[22] Following binarization, a nearest-neighbor boundary smoothing algorithm was applied to smooth pore edges prior to analysis. Binarized images of cross-sections such as these can be imported into shock hydrocodes, such as CTH, to allow for 2D simulations of realistic microstructures.[15-17,23]

Following binarization of the ion-polished cross sections, several microstructure metrics were measured, including average density and local density variations, specific surface area of the porosity, preferred orientation, and two-point correlation functions of the pore phase. While many of these quantities did not display changes with aging beyond that typical of sample-to-sample variation; specific surface area (Fig. 7) and preferred orientation of the porosity did evolve appreciably. Note that it appears that broad beam ion-polishing may induce some degree of "artificial aging" to the PETN, as ion-polished cross-sections of as-deposited films are largely indistinguishable from those of films that had been aged for one day at 60°C, despite clear differences in the morphology observed in both the top surface and fracture cross-section images of these samples.

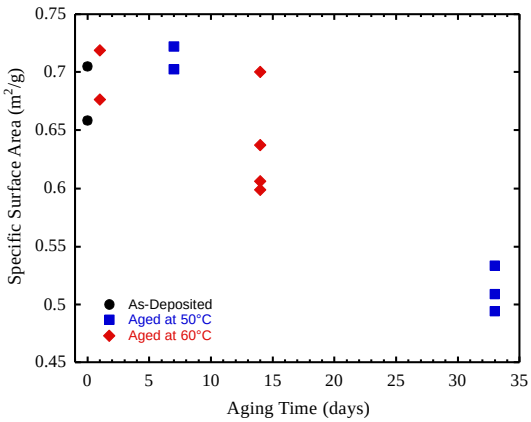

Fig. 6. Plot of specific surface area of the porosity in SEM images of ion-polished PETN cross sections plotted as a function of aging time for films aged at 50°C and 60°C.

It is difficult to determine if there is a correlation between the measured specific surface area and initiation behavior. The values change only subtly over much of the range of the aging conditions tested, and the "as-deposited" ion-polished cross sections likely do not accurately reflect the real microstructure of those samples. While the changes in specific surface area are in the direction one would expect for lower sensitivity with increased aging times, additional work is needed to generate cross-sections of as-deposited samples that better represent the real microstructure in those samples to ascertain if this trend contributes significantly to the observed shifts in performance.

Vapor-deposited PETN films generally contain a low amount of higher molecular weight homologs, such as DiPEHN and TriPEON, compared to typical PETN powders.[10] This is likely due to the deposition process, as higher molecular weight homologs are expected to have lower vapor pressures. This may lead to faster microstructure evolution in these thin film samples than what others have observed with pressed powders, as such impurities may cause diffusional processes to slow due to effects such as solute drag.[24,25] Similar effects have been observed by others,[7,10] where they show that adding a small amount of TriPEON acts as an effective stabilizer for PETN powder.

Conclusions

The combination of vapor-deposited PETN films with the HTI experiment provides a useful model system for investigating the effects of accelerated aging on the evolution of microstructure, chemistry, and performance. The films exhibit considerable grain coarsening early in the aging process, followed by a slower evolution of the porosity following longer times at elevated temperature. This physical change correlates with the trend of decreasing homolog concentration with time/temperature. These changes in microstructure and chemistry result in shifts in both the onset of reaction and transition to detonation to higher flyer impact velocities. This work underscores the importance of developing methods for both controlling and measuring the chemical and physical characteristics of explosives, as even subtle environmental factors can have a significant impact on performance, especially when long periods of time are a factor.

Acknowledgements

The authors would like to thank Adam Pimentel for assistance with ion polishing, Kristin Cochran for performing the UPLC experiments, and Christina Profazi and Jason Phillips for assistance with accelerated aging of the films. This work was supported by the Laboratory Directed Research and Development program at Sandia National Laboratories, a multimission laboratory managed and operated by National Technology & Engineering Solutions of Sandia, LLC (NTESS), a wholly owned subsidiary of Honeywell International Inc., for the U.S. Department of Energy's National Nuclear Security Administration under contract DE-NA0003525. This written work is authored by an employee of NTESS. The employee, not NTESS, owns the right, title, and interest in and to the written work and is responsible for its contents. Any subjective views or opinions that might be expressed in the written work do not necessarily represent the views of the U.S. Government. The publisher acknowledges that the U.S. Government retains a non-exclusive, paid-up, irrevocable, world-wide license to publish or reproduce the published form of this written work or allow others to do so, for U.S. Government purposes. The DOE will provide public access to results of federally sponsored research in accordance with the DOE Public Access Plan.

References

1. Khasainov, B.A., Ermolaev, B.S., Presles, H.N., and Vidal, P., "On the Effect of Grain Size on Shock Sensitivity of Heterogeneous High Explosives" *Shock Waves*, Vol. 7, pp. 89-105, 1997.

2. Howe, P., Frey, R., Taylor, B., and Boyle, V. "Shock Initiation and the Critical Energy Concept" *Sixth Symposium (International) on Detonation*, pp. 11-19, Arlington, VA, 1976.

3. Campbell, A.W., Davis, W.C., Ramsay, J.B., and Travis, J.R., "Shock Initiation of Solid Explosives" *Physics of Fluids*, Vol. 4, pp. 511-521, 1961.

4. Maiti, A. and Gee, R.H., "Modeling Growth, Surface Kinetics, and Morphology Evolution in PETN" *Propellants Explosives Pyrotechnics*, Vol. 34, pp. 489-497, 2009.

5. Maiti, A. and Gee, R.H., "Petn Coarsening - Predictions from Accelerated Aging Data" *Propellants Explosives Pyrotechnics*, Vol. 36, pp. 125-130, 2011.

6. Maiti, A., Shaw, W.L., Clarke, S.M., Fox, C., Ke, L.A., Cheung, W.N., Burton, M.A., Kosiba, G.D., Grant, C.D., and Gee, R.H., "Effect of Thermal Conditioning on the Initiation Threshold of Secondary High Explosives" *Propellants, Explosives, and Pyrotechnics*, Vol. 48, pp. e202300253, 2023.

7. Lease, N., Burnside, N.J., Brown, G.W., Lichthardt, J.P., Campbell, M.C., Buckley, R.T., Kramer, J.F., Parrack, K.M., Anthony, S.P., Tian, H.Z., Sjue, S.K., Preston, D.N., and Manner, V.W., "The Role of Pentaerythritol Tetranitrate (PETN) Aging in Determining Detonator Firing Characteristics" *Propellants Explosives Pyrotechnics*, Vol. 46, pp. 26-38, 2021.

8. Foltz, M.F., "Aging of Pentaerythritol Tetranitrate (PETN)" *Lawrence Livermore National Laboratory Report* 2009.

9. Brown, G.W., Sandstrom, M.M., Giambra, A.M., Archuleta, J.G., and Monroe, D.C., *Thermal Analysis of Pentaerythritol Tetranitrate and Development of a Powder Aging Model*, in *37th Annual Conference of the North American Thermal Analysis Society*. 2009: Lubbock, TX.

10. Maiti, A., Olson, T.Y., Han, T.Y., and Gee, R.H., "Long-Term Coarsening and Function-Time Evolution of an Initiator Powder" *Propellants, Explosives, Pyrotechnics*, Vol. 42, pp. 1352-1357, 2017.

11. Knepper, R., Rupper, S., DeJong, S., Marquez, M.P., Kittell, D.E., Schmitt, R.L., and Tappan, A.S., "Investigating Growth to Detonation in Vapor-Deposited Hexanitrostilbene and Pentaerythritol Tetranitrate Films Using High-Throughput Methods" *Journal of Applied Physics*, Vol. 131, pp. 155901, 2022.

12. Olles, J.D., Wixom, R.R., Knepper, R., and Tappan, A.S., "Observations of Shock-Induced Chemistry with Subnanosecond Resolution"

Applied Physics Letters, Vol. 114, pp. 214102, 2019.

13. Tappan, A.S., Wixom, R.R., and Knepper, R. "Critical Detonation Thickness in Vapor-Deposited Hexanitroazobenzene (HNAB) Films with Different Preparation Conditions" *Fifteenth International Detonation Symposium*, pp. 576-583, San Francisco, CA, 2014.

14. Knepper, R., Marquez, M.P., and Tappan, A.S. "Effects of Confinement on Detonation Behavior of Vapor-Deposited Hexanitrostilbene (HNS) Films" *Sixteenth International Detonation Symposium*, pp. 547-555, Cambridge, MD, 2018.

15. Yarrington, C.D., Kittell, D.E., Bolintineanu, D.S., Lechman, J.B., Wood, M.A., Knepper, R., Olles, J.D., Thompson, A.P., and Wixom, R.R. "Mesoscale Modeling of Explosives at Sandia National Laboratories: Past and Future Directions" *Sixteenth International Detonation Symposium*, pp. 77-87, Cambridge, MD, 2018.

16. Yarrington, C.D., Wixom, R.R., and Damm, D.L., "Shock Interactions with Heterogeneous Energetic Materials" *Journal of Applied Physics*, Vol. 123, pp. 105901, 2018.

17. Molek, C.D., Welle, E.J., Hardin, D.B., Mares, J.O., and Vitarelli, J. "Microstructural Effects on Initiation Behavior of HMX Based Materials" *Sixteenth International Detonation Symposium*, pp. 60-69, Cambridge, MD, 2018.

18. Knepper, R., Tappan, A.S., Wixom, R.R., and Rodriguez, M.A., "Controlling the Microstructure of Vapor-Deposited Pentaerythritol Tetranitrate Films" *Journal of Materials Research*, Vol. 26, pp. 1605-1613, 2011.

19. Dlott, D.D., "Shock Compression Dynamics under a Microscope" *AIP Conference Proceedings*, Vol. 1793, pp. 020001, 2017.

20. Bassett, W.P., Johnson, B.P., Salvati, L., Nissen, E.J., Bhowmick, M., and Dlott, D.D., "Shock Initiation Microscopy with High Time and Space Resolution" *Propellants Explosives Pyrotechnics*, Vol. 45, pp. 223-235, 2020.

21. Levene, H., *Robust Tests for Equality of Variances*, in *Contributions to Probability and Statistics: Essays in Honor of Harold Hotelling*, I. Olkin, Editor. 1960, Stanford University Press: Palo Alto, CA.

22. Kittler, J. and Illingworth, J., "Minimum Error Thresholding" *Pattern Recognition*, Vol. 19, pp. 41-47, 1986.

23. Stewart, J.A., Monti, J.M., Bassett, W.P., Knepper, R., and Damm, D.L. "Effects of Microstructure and Surface Roughness on Initiation Behavior in Vapor-Deposited Explosives" *Seventeenth International Detonation Symposium*, pp. Kansas City, MO, 2024.

24. Hillert, M., "Solute Drag, Solute Trapping and Diffusional Dissipation of Gibbs Energy" *Acta Materialia*, Vol. 47, pp. 4481-4505, 1999.

25. Kirchheim, R., "Grain Coarsening Inhibited by Solute Segregation" *Acta Materialia*, Vol. 50, pp. 413-419, 2002.

Question from Wesley Chapman, Los Alamos National Laboratory

In the ion-polished cross-sections, there is a noticeable seam across the aged samples. Is that an artifact from the coating process or a result of PETN recrystalization?

Answer from Robert Knepper

The seam that is visible in some samples is an artifact of the deposition process. Often, multiple deposition runs are required to reach the desired film thickness. The seam marks a break between deposition runs; a greater amount of porosity is often seen in the vicinity of this break.

Question from Alexander Mueller, Los Alamos National Laboratory

A texture similar to the one seen throughout fracture cross-section of the sample aged at 70°C for 1 month can be observed near the PETN-substrate interface of the 60°C aged samples. Have there been initiation measurements on films in an inverted geometry to see if this changes the degradation in sensitivity?

Answer from Robert Knepper

This is an interesting idea – to remove the film from the substrate and initiate from the back side. We

have not performed experiments like this to date. Generally, vapor-deposited PETN films have a higher density (less porosity) near the substrate interface and develop greater porosity as the film grows thicker (see ref 18). As such, one would expect that the films would generally be less sensitive when initiating from the back side. From the available data, it is unclear if this trend in porosity remains following aging at 70°C for 1 month or if the distribution of porosity has become more uniform across the thickness of the film. Ion-polished cross-sections of films aged at lesser time/temperature conditions show this trend persisting. As such, I would expect the trends in initiation measured here to largely remain when initiating from the back side of the sample, just with a somewhat less sensitive starting condition. It is unclear how the sample aged at 70°C for 1 month would behave when impacted from the back side, as the effects of grain and pore coarsening could be competing with the effects of greater overall porosity near the impact site.

Question from Timothy Ransom, Office of Naval Research

How does the information on this model system help us more broadly understand aging effects?

Answer from Robert Knepper

The UPLC data indicate that chemical changes to the samples are minimal over the range of aging conditions tested here. That, in turn, suggests that the measured changes in performance are due to the evolution of microstructure. Thus, if these changes in microstructure can be measured or predicted, changes in performance due to aging can potentially be predicted as well using techniques like mesoscale simulations that directly capture the effects of microstructure.